

Final Draft
of the original manuscript:

Zhou, H.; Steinhilber, D.; Schlaad, H.; Sisson, A.L.; Haag, R.:
**Glycerol based polyether-nanogels with tunable properties via
acid-catalyzed epoxide-opening in miniemulsion**
In: Reactive and Functional Polymers (2010) Elsevier

DOI: 10.1016/j.reactfunctpolym.2010.11.018

Glycerol based polyether-nanogels with tunable properties via acid-catalyzed epoxide-opening in miniemulsion

Haixia Zhou^a, Dirk Steinhilber^a, Helmut Schlaad^b, Adam Sisson^c, Rainer Haag^{a*}

^aInstitut für Chemie and Biochemie, Freie Universität Berlin, Takustr. 3, 14195 Berlin, Germany

^bMax Planck Institute of Colloids and Interfaces, Dept. of Colloid Chemistry, Research Campus Golm, 14424 Potsdam, Germany

^cBerlin-Brandenburg Center for Regenerative Therapies, Augustenburger Platz 1, 13353 Berlin, Germany

GKSS Forschungszentrum Geesthacht, Kantstrasse 55, 14513 Teltow-Seehof, Germany

*Corresponding author. Address: Institut für Chemie and Biochemie, Freie Universität Berlin, Takustr. 3, 14195 Berlin, Germany

Tel: +49-30-838-52633(direct)+49-30-838-53358(secretary)

Fax. +49-30-838-53357

E-mail: haag@chemie.fu-berlin.de

Abstract

A series of defined nanogels of 20-120 nm in diameter were synthesized by acid-catalyzed epoxid-opening polymerization based on glycerol in miniemulsion. Multifunctional alcohols were used as monomers and di- and triepoxides as crosslinking agents. The properties of these nanogels, i.e., size, degree of branching, viscosity, and swelling behavior, can be controlled by varying the functionalities of the monomers and crosslinkers. Inverse gated ^{13}C -NMR indicated that the addition of monomer occurred at both ends of the opened epoxide ring of the crosslinkers. This feature led to higher degree of branching and consequently to a lower viscosity of the resulting nanogels. The formation of some cycles as a possible side reaction was evidenced by different particle sizes in dry (TEM) and swollen states (DLS in water).

Keywords

Glycerol based nanogel, inverse miniemulsion, watersoluble nanogels intrinsic viscosity, degree of branching, particle size

1. Introduction

Over the last decade hyperbranched aliphatic polyethers have gained widespread attention because of their high biocompatibility and solubility in water [1, 2]. These macromolecules typically exhibit compact, globular structures in combination with a high number of functional groups. Therefore a wide range of applications have been foreseen for them in biomedical science, which include solubility enhancement, MRI contrast agents, neutron capture therapy, gene therapy, drug delivery, and photodynamic therapy [3,4]. Water soluble hyperbranched polyglycerols (hPGs), which are built of glycerol units, have played a major role here.

In 1999 Sunder et al. reported the use of latent AB_2 monomers for a ring-opening multi-branching polymerization following single monomer methodology (SMM) which is based on polymerization of AB_x -type monomers [5]. Polymerization of such monomers results in highly branched polymers, as long as A only reacts with B from another molecule. Intramolecular reaction between A and B results in termination of polymerization by cyclization [6]. This technique is interesting for polymer chemistry, because it hinders the formation of by-products. PG with the highest number-average molecular weight of 700 kDa and a particle size of approximately 10 nm were reported by Brooks et al. in 2006 [7]. In 2009 Frey et al. achieved a molecular weight of 24 kDa in a two-step approach using a low molecular weight PG with low polydispersity index (PDI) as a macroinitiator [8].

Particles ranging in size from 20-100 nm, however, are desired for several biomedical applications [1,3]. The above-mentioned approaches show that classical methods do not yield particles of the required size [9,10]. Thus the PG synthesis needs to be extended to larger polyether particles with controlled physical properties. Recently, our group reported polyglycerol nanogels with controllable sizes that were between 25 and 85 nm in diameter using inexpensive, commercially available monomers [11,12] or dendritic precursors [13] in miniemulsion. Degradable particles have also been obtained [14]. These nanogels are completely soluble in polar solvents including water and show promising results in cellular uptake studies due to their defined size and high biocompatibility.

Unlike the classical SMM based on glycidol, we followed the double monomer methodology (DMM), which was first reported in the work of Kakimoto [15] and Fréchet [16] on hyperbranched polymers via the A_2+B_3 approach. We recently extended this approach to A_n and B_m . Copolymerization of A_n and B_m or other

multifunctional monomers can also give rise to hyperbranched polymers, provided that the polymerization is kept below the gel point by limiting polymer conversion or by manipulation of the multifunctional monomer stoichiometry [6,17,18]. Exceeding the critical condition leads to undesired gelation, which can become beneficial when controlled by miniemulsion techniques.

Miniemulsions are specially formulated heterophase systems consisting of nanodroplets in a continuous phase. They can be fabricated by shearing a system containing two immiscible liquids, a surfactant, and an osmotic pressure agent, which is soluble in the dispersed phase but not in the continuous phase [19]. After rapid stirring and treatment with a sonicator the mixture becomes a dispersion containing rather monodisperse droplets of 50-500 nm in diameter [11,13]. Each droplet acts as a discrete nanoreactor vessel, in which polymerization takes place. The resulting polymer particles ought to represent 1:1 copies of the dispersed droplets [20]. This last feature allows a wide range of well-defined materials to be prepared in an efficient way. (Fig. 1).

Nanoparticles with unique physical properties have been shown to influence many vital interactions with the body including phagocytosis, circulation, targeting, and adhesion [21]. We have recently demonstrated that PG nanogels of 20-50 nm have ideal particle sizes for cellular uptake.

Here we report on the physical properties of polyether nanogels. For this purpose a series of branched polyethers has been synthesized by crosslinking a mixture of A_n and B_m building blocks as monomer and crosslinking agents respectively in miniemulsion in order to obtain nanogels with properties that are tunable and suited for different applications.

2 Experimental Section

2.1 Materials.

General chemicals were purchased from Acros Organics and Raschig. The water used was Millipore filtered.

Poly(ethylene-co-butylene)-*block*-poly(ethylene oxide) (KLE = **K**raton **L**iquidTM-*block*-**P**EO, number-average molecular weight: 8.1 kDa, 41 wt% PEO), was prepared and used according to published procedures [22, 23]. Emulsions were sonicated using a sonicator, W-220f, with microtip on 70% intensity (company: Heat Systems-

Ultrasonics, Inc.) Transmission electron microscopy samples were prepared on copper grids (200 mesh) by blotting samples in 1% aqueous phosphotungstic acid and visualized using a Philips CM12 electron microscope. Dynamic light scattering measurements were conducted using a BioDLS particle sizer (Brookhaven Instruments Corp.) The viscosity measurements of the nanogels were performed by a Schott Ubbelohde viscometer. The viscosities of aqueous solutions of concentrations ranging from 1 to 10 mg/mL were measured at 37 °C. Plotting η_{sp}/c versus c revealed their intrinsic viscosity $[\eta]$. Each measurement was repeated at least three times to calculate the average value. Estimation of OH amount were performed by titration according to DIN 53240-2.

^1H -NMR and inverse gated ^{13}C -NMR spectra were recorded on a Bruker AV 700 (700 MHz for ^1H , 176 MHz for ^{13}C) instrument. Samples were dissolved in CD_3OD and measured at room temperature. Chemical shifts δ are given in ppm relative to TMS as an internal standard or relative to the resonance of the solvent (^1H NMR: methanol: $\delta = 3.34$ ppm ^{13}C NMR: methanol: $\delta = 49.05$ ppm). Inverse gated ^{13}C -NMR were performed with following parameter: delay time = 10 s, acquisition time = 0.78 s, number of scans = 1024-4096, depending on sample concentration (80-250 mg in 0.7 mL solvent).

2.2 General procedure for the preparation of particles 1-7 (example given for product 1).

A solution of the KLE surfactant (20 mg, 0.0025 mmol) in cyclohexane (15 mL) was vigorously stirred in a cylindrical 30-mL vial for 30 min. A mixture of A_n , B_m , and 0.2 mL DMSO was added to the cyclohexane phase. The amount of A_n and B_m was calculated so that the ratio between the hydroxyl and epoxide groups was 3:2 and the total mass of A_n and B_m was 1 g. The mixture was stirred vigorously for 1 h.

Afterwards a slightly turbid macroemulsion was formed, which would have otherwise rapidly separated. The formed macroemulsion was ultrasonicated for one minute with a sonic tip apparatus four times under water cooling to form a fully homogenous miniemulsion. (The resultant miniemulsion was stable for several hours.) The miniemulsion was transferred to the resealable tube charged with a catalytic amount of para-toluene sulfonic acid (p-TSA). The miniemulsion was heated under stirring at 120 °C for 16 h. Finally the reaction was quenched with water and heated for 2 h.

After cooling to room temperature, the nanogels were precipitated as a honey like mass upon addition of n-hexane (30 mL). They were then purified from the surfactant by solid/liquid extraction, which was performed three times with n-hexane. Separation of the product from lower molecular impurities was carried out by ultracentrifugation in ultracentrifuge tubes with 10 kDa MWCO. Yields of isolated polymer ranged between 10% and 50%.

$^1\text{H-NMR}$ (CD_3OD , 700 MHz): δ (ppm) = 4.00-3.40 (m, PG backbone). $^{13}\text{C-NMR}$ (CD_3OD , 176 MHz): δ (ppm) = 62.6 (L_{13} , CH_2OH); 64.4(T, CH_2OH); 70.6 (L_{13} , CH_2); 70.7 (L_{14} , CHOH); 72.2 (T, CHOH and CH_2); 72.2 (D, CH_2); 73.9 (L_{14} , CH_2); 80.3 (D, CH); 81.5 (L_{13} , CH).

3. Results and Discussion

3.1 Synthesis

The synthesis of the nanogels was performed according to the procedure described above. The reaction is illustrated schematically in Fig. 2. Different combinations of A_n and B_m building blocks are listed in Tab. 1. The applied reaction is based on a polyaddition of an alcohol to an epoxide by acid catalysis. The nanogels were synthesized from cheap and commercially available glycerol/oligoglycerols as monomers and bis- /trisepoxides as crosslinker.

Base-catalyzed polyaddition of aromatic bis-alcohol to bis-epoxide performed in miniemulsion has already been reported by Landfester et al [24]. In our case, the acid catalyzed reaction required higher temperatures, i.e. 120 °C. In order to stabilize the emulsion against Ostwald ripening, which can cause monomer diffusion from small to big droplets, DMSO was used as osmotic pressure agent [19,25]. In the presence of the non-ionic copolymer surfactant KLE a controlled particle size of highly branched (random network) polyether polyol nanogel was obtained (Fig. 2). An approach without osmotic pressure agent led to formation of crosslinked polymer network on the macroscale, which was insoluble [25].

3.2 Inverse gated ^{13}C NMR analysis

Analysis of PG by signal assignments for $^{13}\text{C-NMR}$ spectra was first reported by Vandenberg [26] and later extended by Penczek [27] and Dworak [28]. Calculation of the degrees of branching, however, was only possible after Frey utilized inverse gated $^{13}\text{C-NMR}$ technique [5] to obtain quantitative ^1H decoupled $^{13}\text{C-NMR}$ spectra.

Due to the low abundance and small magnetic moment of the ^{13}C nucleus, the signals are only visible by coupling with ^1H nuclei in their environment. As a result, the intensities of the signals were highly dependent on the ^1H nuclei which are bound to C, and did not reflect the quantitative ratio of the carbon atoms. The technique of inverse gated ^{13}C -NMR, however, produced carbon signals of high qualities despite the decoupling of ^1H , because of long delay time up to 10 s and high number of scans. Under these conditions, one observes ^{13}C -NMR signals with intensities corresponding to the carbon ratio [29].

Since the dendritic, linear and terminal carbons caused signals with different chemical shifts, their inverse gated ^{13}C -NMR spectrum offered the opportunity to calculate the degree of branching [4, 5],

PGs prepared by Frey and Brooks, as well as our nanogels, possess seven well resolved peak regions between 60-85 ppm that originate from dendritic, linear, and terminal polyether units. All signals can be assigned as given in Fig. 3: (i) linear 1,3-unit (L_{13}): CH_2OH carbon at 62.6 ppm; CH_2 carbon at 70.6 ppm and CH carbon at 81.5 ppm; (ii) linear 1,4-unit (L_{14}): both CH_2 carbons at 73.9 ppm, CHOH carbon at 70.7 ppm ; (iii) terminal unit (T): CH_2OH carbon at 64.4 ppm, CHOH carbon at 72.2 ppm, and the CH_2 carbon at 72.2 ppm; (iv) dendritic unit (D): CH carbon at 80.3 ppm, two CH_2 carbons at about 72.2 ppm overlapping with a CH_2 carbon of a terminal unit [5]. These peaks provide information about the compactness of the structure. In simple systems like nanogel **1**, one can even calculate the ratio of the crosslinker by assigning the spectra. Here we used this quantitative analysis method to determine the degrees of crosslinking by calculating the fraction of dendritic units involved in the network. The structure and the inverse gated ^{13}C -NMR spectrum of nanogel **1** are also shown in Fig. 3. Carbons belonging to the terminal, dendritic, linear 1,3 and linear 1,4 units are indicated by T, D, L_{13} , and L_{14} , respectively.

3.3 Degree of crosslinking and degree of branching

The degree of crosslinking (DC), defined as the number of crosslinks per monomer, is mostly determined as the reciprocal of the degree of swelling, which can be measured by swelling in a respective solvent [30]. In some cases it can be calculated based on NMR data [31]. These calculations, however, are more suited for networks consisting of long chain polymers.

Concerning their monomers, these nanogels can also be considered as hyperbranched polyglycerols, because every unit reacted with crosslinker resulted in a dendritic unit. Therefore their degrees of crosslinking can be correlated with the degree of branching (DB).

In general the DB may be calculated according to Fréchet (DB₁) or Frey (DB₂) by the following equations [5,32,33] .

$$DB_1 = \frac{D+T}{D+T+L} \quad (1)$$

$$DB_2 = \frac{2D}{2D+L} \quad (2)$$

T, L, and D designate the terminal units, non-branched linear units, and fully branched, dendritic units, respectively. For polymers with relatively low molecular weight, Fréchet's calculation involving the terminal units overestimates the DB values. The equation according to Frey, however, leads to lower DB values. For large polymers, like the nanogels treated here, both equations are suitable. By means of the inverse gated ¹³C-NMR, the DB value can be calculated as follows:

$$DB = \frac{2D}{2D + L_{13} + L_{14}} \quad (3)$$

The branching in our case was "diluted" by an increased number of linear units of the monomer and in greater distances between the branching. The DB value of a hyperbranched polyglycerol typically ranges between 0.5-0.6 [34], and the highest possible DB value of a simple HPG is 0.666. The DB value of a linear polymer is 0.

The results for the degree of branching of each nanogel are summarized in Fig. 4. The first product synthesized was nanogel **2** based on an A₃+B₃ system consisting of glycerol and glycerol tris-glycidyl ether (GTGE). This approach provided us a degree of branching of 0.63, close to the highest possible value. By extending the series nanogel **1** based on A₂+B₃ system was obtained with a slightly higher DB value of 0.64. These values are rather high compared to the HPGs reported by Frey and Brooks with DBs of 0.5-0.6 [6, 8]. Also a significant difference between the DB values of A₂+B₃ (ethylene glycol + GTGE) and A₃+B₂ (glycerin + DGE with DB of 0.27) was observed, which indicated a stronger impact of crosslinker on DB. On the one hand this impact can be explained by the mechanism of the ring-opening reaction, in which the epoxid is the reaction deciding component. On the other hand, the epoxide rings act as potential branching points, which led to higher DB. Furthermore one can

suppose that after the ring opening both ends reacted with monomer. This presumption may also be revealed by the calculation of the crosslinker/monomer ratio by means of ^{13}C -NMR. If we assume that the ring-opening polymerization is quantitative (reaction **a** in Scheme 1) the peak at $\delta = 80$ ppm caused by the dendritic units may be solely attributed to the CH-carbon of the GTGE. Accordingly, D is a direct measure of the fraction of fully reacted crosslinker B_m . In this case, the ratio between crosslinker and monomer could be simply calculated as

$$\frac{n_{\text{monomer}}}{n_{\text{crosslinker}}} = \frac{\text{total} - 12D}{2D} \quad (4)$$

The calculation shows that the fraction of D was, however, much higher than expected. This can be explained by the occurrence of reaction **b** in Scheme 1, and leading to a high degree of branching. Furthermore, macrocycles may also be formed (reaction **c** in Scheme 1).

Motivated by these promising approaches, we investigated more systems based on oligoglycerol and multifunctional alcohols aiming increase the degree of branching.

However, contrary to expectation, oligoglycerol with a larger number of OH moieties did not lead to a higher DB value (Fig. 3b). This can be partially explained by reduced activity of secondary alcohols. The main reason, however, is the average number of branches (\overline{NB}). It is not possible, at least in a random process, to enhance the “density of branching” beyond a threshold value by using monomers with higher functionality [33]. The \overline{NB} for an AB_m -system is expressed as

$$\overline{NB} = \left[\left(\frac{m}{m-1} \right)^m - 1 \right]^{-1} \quad (5)$$

For the A_2+B_2 system there was just a tiny peak at $\delta = 80$ ppm in ^{13}C -NMR spectrum (Fig. 3c) caused by dendritic C-H units. Dendritic units appear to be absent indicating the presence of a linear polymer.

3.4 Intrinsic viscosity $[\eta]$

Hyperbranched polymers as well as the glycerol based nanogels described in this work are generally globular in shape. The absence of entanglements is expected to lead to lower viscosities as compared to linear polymers. Furthermore, the nanogels

could be applied at high concentration without a dramatic increase of the solution viscosity – this property is of great biomedical importance [35].

The intrinsic viscosity was determined by measuring specific viscosities of diluted aqueous solutions at different concentrations followed by linear extrapolation to zero concentration. It is worth to mentioned that nanogel **1** (DB = 0.64) contains 11.2 mmol/g hydroxyl groups, which is close to number reported for classical hPG, as determined by titration. Nanogel **7** with the lowest DB value (0.04) carries 5.8 mmol/g OH groups. The differences in hydroxyl numbers may have impact on strength of hydrogen bonding interactions of the materials. However, hydrogen bonding should not disturb the measurements of intrinsic viscosity because of the low concentration of the substance.

As shown in Fig. 5, the intrinsic viscosity decreased with an increasing degree of branching, but did not depend on the particle size. The viscosity showed an almost linear behavior in correlation with the DB value. Accordingly, it is possible to predict the viscosity based on DB, which can be controlled by the ratio of monomer to crosslinker ratios. The lowest intrinsic viscosity of 1.6 mL/g was detected for nanogel **1**, with the highest degree of branching. Compared to the hPGs with DB values of 0.5-0.6 and intrinsic viscosity of 2.2 mL/g reported by Brooks, nanogel **1** exhibited a lower viscosity although the particles were much larger in size [7]. One of the potential uses of this class of nanogel is as plasma expanders which are typically infused at higher concentrations [35]. Nanogels with low degrees of branching, like nanogels **5** and **7**, show similar viscosities as linear PEG, which can be attributed to entanglements [25].

3.5 Particle sizes and swelling properties

The nanogels may contain cycles, formed by linear monomer according to the reaction path **c** (Scheme 1), which can affect nanogel properties like swelling. As no small cycles were observed by NMR, the degree of swelling was analyzed, which can be expressed as the reciprocal of the degree of crosslinking and is inversely proportional to the number of cycles. Usually it is measured as $m_{\text{absorbed solvent}} / m_{\text{polymer}}$. Because of the physical characteristics of such waxy products however, the swelling property of the nanogel could not be measured this way. Therefore changes in the particle sizes between dry and swollen states had to be investigated.

Fig. 6 shows the different particle sizes of nanogel **1** in the dry state and in solution. Dynamic light scattering (DLS) analysis of an aqueous nanogel solution

revealed particles being about 100 nm in diameter. The same sample measured with transmission electron microscopy (TEM) under high vacuum conditions showed much smaller particle sizes in the range of $27 \text{ nm} \pm 15\%$. This volume difference indicated a significant swelling of nanogel particles in water and can be expressed as $\Delta V/V_{\text{dry}}$. For this example the swelling factor was ~ 30 .

The particle sizes of nanogel **2**, consisting of an A_3+B_3 system, measured in the hydrated and in the dry state were found to be very similar [11]. Accordingly, nanogel **2** is less swellable and contains more cyclic units than nanogel **1**. This feature could not be recognized by investigating viscosity because branching as well as cyclization lead to a more compact structure and consequently to a lower viscosity. Cycle formation is only accessible by their swelling behavior.

DLS measurement revealed defined correlation curves, which implied a narrow particle size distribution and spherical shape of the sample which is confirmed by correlation function. By TEM, however, one could see elongated particles, which may have been either formed by collision of the droplets or by aggregation of two or more particles because of the drying effect.

4. Conclusion

A series of defined glycerol based nanogels with sizes between 20-120 nm in diameter were synthesized by miniemulsion polymerization. The investigation of several physical properties like degree of branching, size, viscosity, and swelling properties show a clear structure property correlation. Since glycerol based nanogels already showed good biocompatibility, these properties will be useful for a number of biomedical applications such as plasma expanders, drug delivery or medical imaging.

This work presented a way to synthesize glycerol based nanogels with predictable properties. In our ongoing work, we want to use these tailor-made particles for cellular studies.

Acknowledgements We would like to thank Ines Below-Lutz for the synthesis of KLE and Andrea Schulz for the TEM measurements. The authors thank the Deutsche Forschungsgemeinschaft and SFB 765 for financial support.

References

- [1]. H. Frey, R. Haag, Dendritic polyglycerol: a new versatile biocompatible material, *Rev. Mol. Biotech.* 90 (2002) 257-267.
- [2]. D. Wilms, S.-E. Stiriba, H. Frey, Hyperbranched polyglycerols: from the controlled synthesis of biocompatible polyether polyols to multipurpose applications, *Accounts Chem. Res.* 43 (2009) 129-141.
- [3]. R. Haag; M. Calderon; M.A. Quadir; S.K. Sharma, Dendritic polyglycerols for biomedical applications, *Adv. Mater.* 22 (2010) 190-218.
- [4]. R. Mülhaupt; A. Sunder, R. Haag, H. Frey, Hyperbranched Polyether Polyols: A modular approach to complex polymer architectures, *Adv. Mater.* 12 (2000) 235-239.
- [5]. A. Sunder, R. Hanselmann, H. Frey, R. Mülhaupt, Controlled Synthesis of hyperbranched polyglycerols by Ring-Opening Multibranching Polymerization, *Macromolecules* 32 (1999) 4240-4246.
- [6]. C. Gao, D. Yan, Hyperbranched polymers: from synthesis to applications, *Prog. Polym. Sci.* 29 (2004) 183-275.
- [7]. R.K. Kainthan, E.B. Muliawan, S.G. Hatzikiriakos, D.E. Brooks, Synthesis, characterization, and viscoelastic properties of high molecular weight hyperbranched polyglycerols, *Macromolecules* 39 (2006) 7708-7717.
- [8]. D. Wilms, F. Wurm, J.R. Nieberle, P. Böhm, U. Kemmer-Jonas, H. Frey, Hyperbranched Polyglycerols with Elevated Molecular Weights: A facile Two-Step Synthesis Protocol Based on Polyglycerol Macroinitiators, *Macromolecules* 42 (2009) 3230-3236.
- [9]. B. Voit, Hyperbranched polymers-All problems solved after 15 years of research?, *J. Polym. Sci. Part A: Polym. Chem.* 43 (2005) 2679-2699.
- [10]. A.L. Sisson, R. Haag, Polyglycerol nanogels: highly functional scaffolds for biomedical applications *Soft Matter* DOI: 10.1039/c0sm00149j (2010)
- [11]. A.L. Sisson, D. Steinhilber, T. Rossow, P. Welker, K. Licha, R. Haag, Biocompatible functionalized polyglycerol microgels with cell penetrating properties, *Angew. Chem. Int. Edit.* 48 (2009) 7540-7545.
- [12]. A.L. Sisson. R. Haag, D. Steinhilber, H. Zhou, Method for producing crosslinked polyglycerol based nanoparticles, nanoparticle systems and their use, patent WO2009156455 (2009)
- [13]. A.L. Sisson, I. Papp, K. Landfester, R. Haag, Functional nanoparticles from dendritic precursors: hierarchical assembly in miniemulsion, *Macromolecules* 42 (2008) 556-559.
- [14]. A.L. Sisson. D. Steinhilber, D. Mangoldt, P. Welker, K. Licha, R. Haag Synthesis, Reductive Cleavage, and Cellular Interaction studies of biodegradable polyglycerol Nanogels *Adv. Func. Mater.* accepted (2010)
- [15]. M. Jikei, S.-H. Chon, M.-A. Kakimoto, S. Kawauchi, T. Imase, J. Watanebe, Synthesis of hyperbranched aromatic polyamide from aromatic diamines and trimesic acid, *Macromolecules* 32 (1999) 2061-2064.
- [16]. T. Emrick, H.-T. Chang, J.M.J. Fréchet, An A₂ + B₃ approach to hyperbranched aliphatic polyethers containing chain end epoxy substituents, *Macromolecules* 32 (1999) 6380-6382.
- [17]. Y.H. Kim, Hyperbranched polymers 10 years after, *J. Polym. Sci. Part A-Polym. Chem.* 36 (1998) 1685-1698.
- [18]. K. Landfester, Miniemulsion polymerization and the structure of polymer and hybrid nanoparticles *Angew. Chem. Int. Ed.* 48 (2009) 4488-4507

- [19]. K. Landfester, Miniemulsions for nanoparticle synthesis, *Top. Curr. Chem.* 227 (2003) 75-123.
- [20]. M. Antonietti, E. Wenz, L. Bronstein, M. Seregina, Synthesis and characterization of noble metal colloids in block copolymer micelles, *Adv. Mater.* 7 (1995) 1000-1005.
- [21]. S. Mitragotri, J. Lahann, Physical approaches to biomaterial design, *Nature Materials* 8 (2009) 15-23.
- [22]. A. Thomas, H. Schlaad, B. Smarsly, M. Antonietti, Replication of lyotropic block copolymer mesophases into porous silica by nanocasting: learning about finer details of polymer self-assembly, *Langmuir* 19 (2003) 4455-4459.
- [23]. J.K. Oh, H. Dong, R. Zhang, K. Matyjaszewski, H. Schlaad, Preparation of nanoparticles of double-hydrophilic PEO-PHEMA block copolymers by AGET ATRP in inverse miniemulsion, *J. Polym. Sci. Part A: Polym. Chem* 45 (2007) 4764-4772.
- [24]. K. Landfester, F. Tiarks, H.P. Hentze, M. Antonietti, Polyaddition in miniemulsions: A new route to polymer dispersions, *Macromolecular Chem. Physic.* 201 (2000) 1-5.
- [25]. D. Steinhilber, Master thesis, Freie Universität Berlin (2008)
- [26]. E.J. Vandenberg, Polymerization of glycidol and its derivatives: A new rearrangement polymerization, *Journal of Polymer Science: Polymer Chemistry Edition* 23 (1985) 915-949.
- [27]. R. Tokar, P. Kubisa, S. Penczek, A. Dworak, Cationic polymerization of glycidol: coexistence of the activated monomer and active chain end mechanism, *Macromolecules* 27 (1994) 320-322.
- [28]. A. Dworak, W. Walach, B. Trzebicka, Cationic polymerization of glycidol. Polymer structure and polymerization mechanism, *Macromolecular Chem. Physic.* 196 (1995) 1963-1970.
- [29]. P. Giraudeau, J.L. Wang, É. Baguet, Improvement of the inverse-gated-decoupling sequence for a faster quantitative analysis by ¹³C NMR, *C. R. Chimie* 9 (2006) 525-529
- [30]. G. Jiang, C. Liu, X. Liu, G. Zhang, M. Yang, Q. Chen, F. Liu, Swelling behavior of hydrophobic association hydrogels with high mechanical strength, *J. Macromol. Sci., Part A: Pure and Applied Chemistry* 47 (2010) 662-677
- [31]. M.A. Gauthier, J. Luo, D. Calvet, C. Ni, X.X. Zhu, M. Garon, M.D. Buschmann, Degree of crosslinking and mechanical properties of crosslinked poly(vinyl alcohol) beads for use in solid-phase organic synthesis, *Polymer* 45 (2004) 8201-8210.
- [32]. D. Hölter, A. Burgath, H. Frey, Degree of branching in hyperbranched Polymers, *Acta. Polymer.* 48 (1997) 30-35.
- [33]. C.J. Hawker, R. Lee, J.M.J. Fréchet, One-Step synthesis of hyperbranched dendritic polyesters, *J. Am. Chem. Soc.* 113 (1991) 4583-4588.
- [34]. J.M.J. Fréchet, C.J. Hawker, I. Gitsov, J.W. Leon, Dendrimers and hyperbranched polymers: two families of three-dimensional Macromolecules with similar but clearly distinct properties, *J. Macromol. Sci. Pure Appl. Chem.* A33 (1996) 1399-1425
- [35]. R.K. Kainthan, D.E. Brooks, In vivo biological evaluation of high molecular weight hyperbranched polyglycerols, *Biomaterials* 28 (2007) 4779-4787.

Figure Captions

Figure 1. Schematic representation of the synthesis of glycerol based nanogels via inverse miniemulsion.

Figure 2. Principle of miniemulsion polymerization reactions based on A_n and B_m in the presence of a copolymer surfactant leading to controlled polyether polyol nanogels.

Figure 3 Nanogel based on glycerol trisglycidylether and ethylene glycol.

Left: Structure of nanogel **1**.

Right: a) Inverse gated ^{13}C -NMR spectrum of nanogel **1**, b) inverse gated ^{13}C -NMR spectrum of nanogel **6** based on A_5+B_3 system, c) inverse gated ^{13}C -NMR spectrum of non-branched nanogel based on A_2+B_2 systems.

Figure 4. Degrees of nanogel branching **1-7** calculated based on inverse gated ^{13}C -NMR measurements.

Figure 5. Plot of the intrinsic viscosity versus the degree of branching of the nanogel.

Figure 6. Particle size distributions of nanogel **1** measured by dynamic light scattering (DLS) in water (right) and by TEM under dry condition (left).

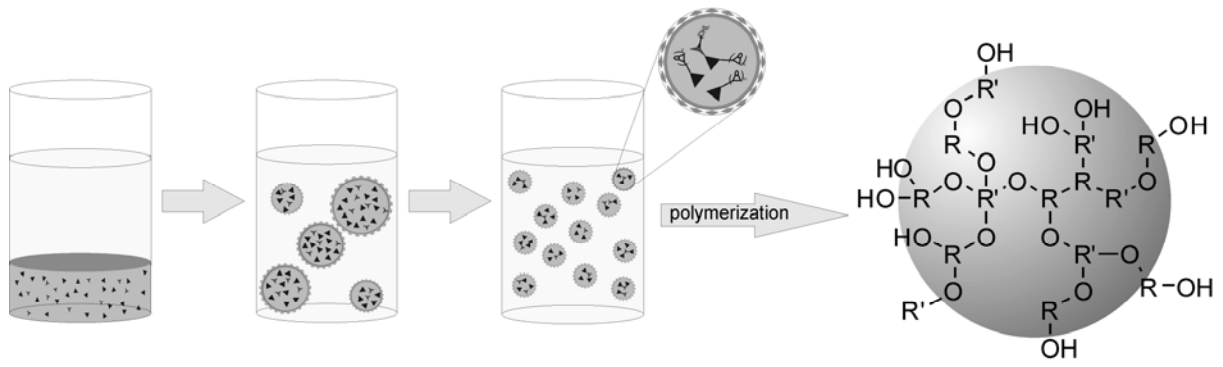


Figure 1

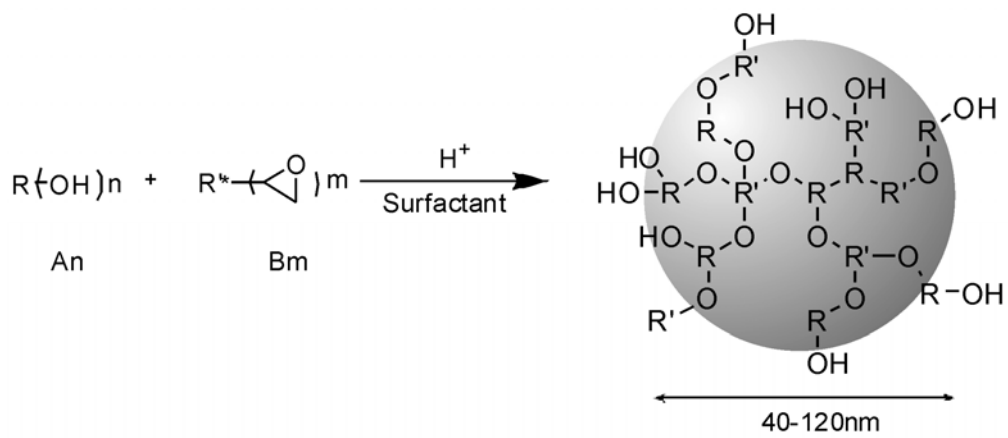


Figure 2

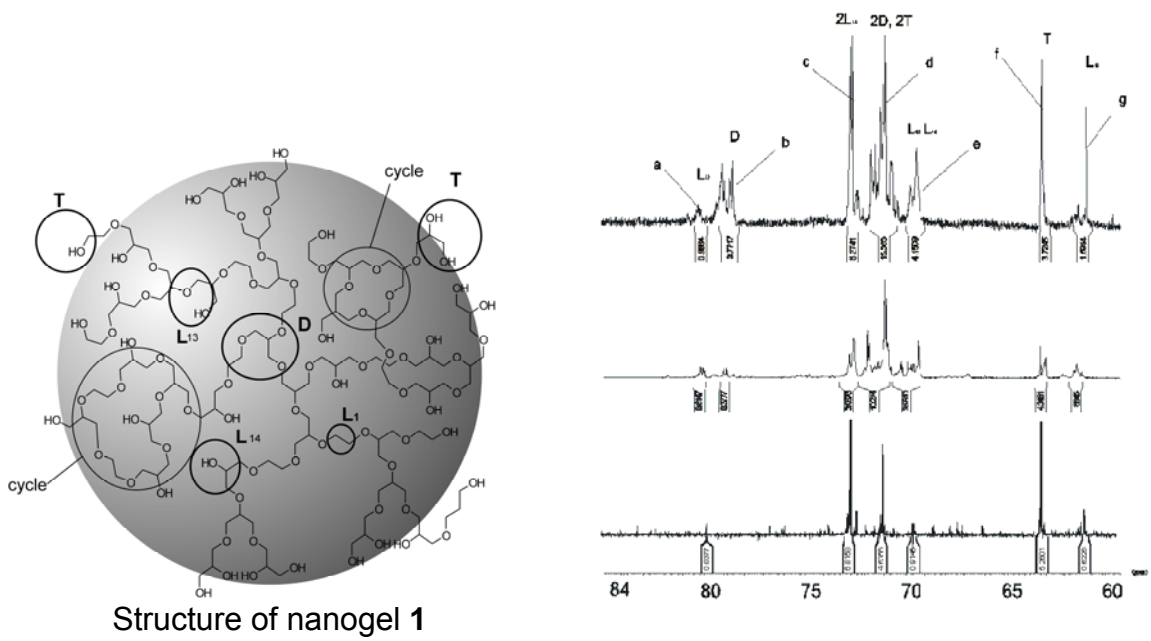


Figure. 3

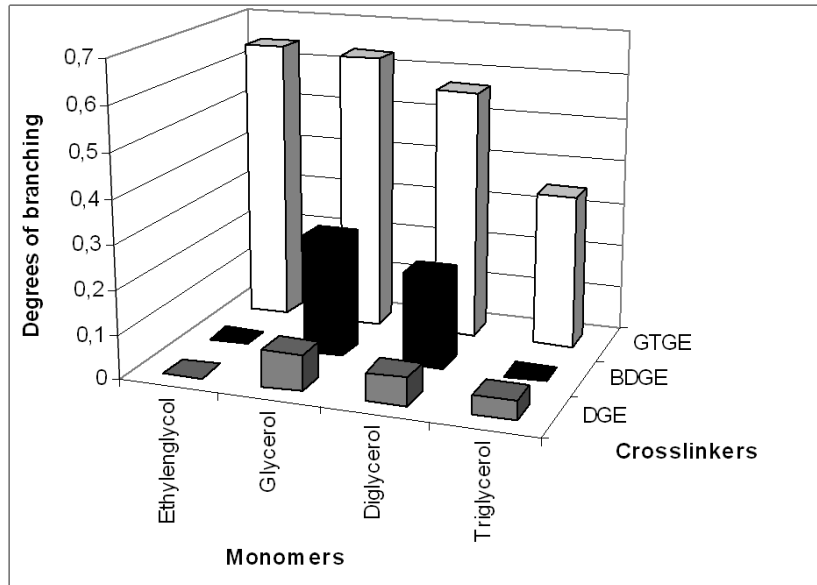


Figure. 4

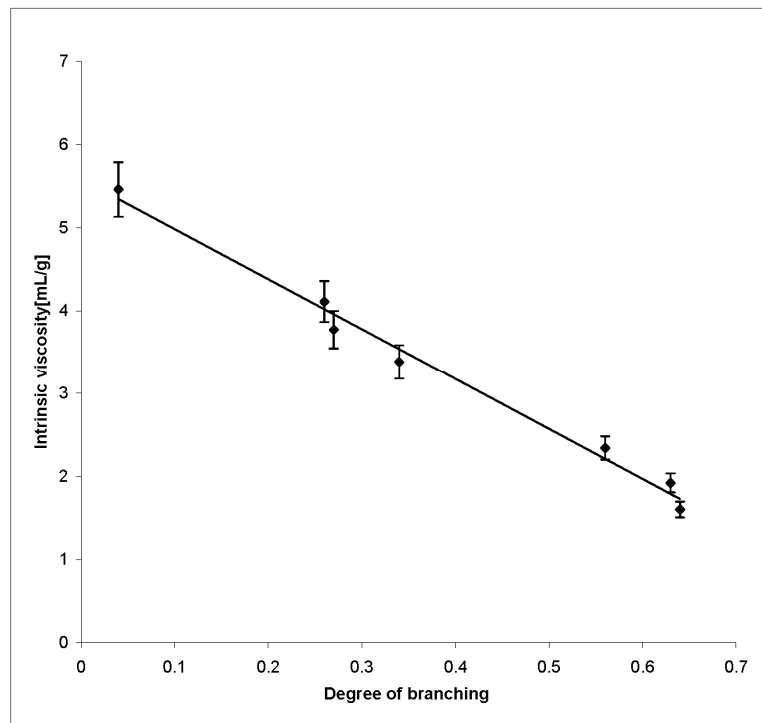


Figure. 5

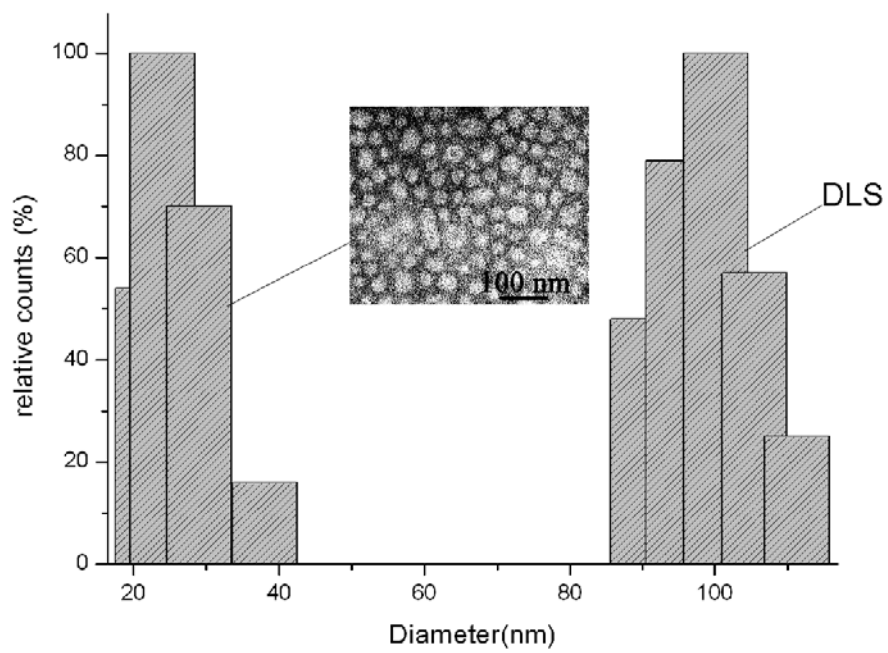
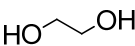
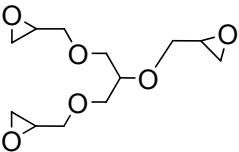
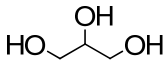
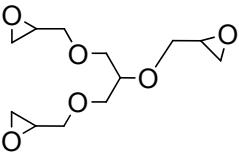
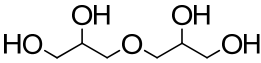
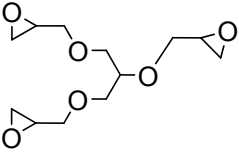
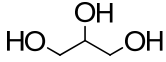
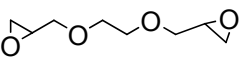
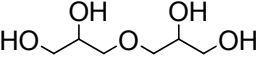
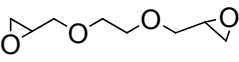
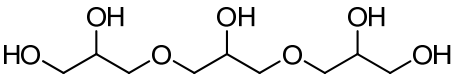
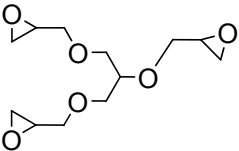
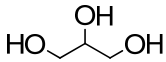
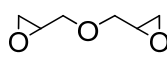


Figure. 6

Table 1. Nanogel synthesis from $A_n + B_m$ monomers via miniemulsion polymerization and some physical data.

System	A_n	B_m	DB	Diameter ^a (nm)	Intrinsic viscosity ^b (mL/g)
1 A_2+B_3			0.64	100	1.6
2 A_3+B_3			0.63	45	1.92
3 A_4+B_3			0.57	43	2.34
4 A_3+B_2			0.27	116	3.77
5 A_4+B_2			0.06	73	4.11
6 A_5+B_3			0.35	50	3.38
7 A_3+B_2			0.04	75	5.46

^a measured by dynamic light scattering in water with a Zetasizer Nano ZS machine

^b measured with a Ubbelohde viscometer in aqueous solution at 37°C